

electric locomotive; asynchronous traction drive;  
computer modeling of electro-mechanical processes

**Pavel KOLPAHCHYAN\***, Alexander ZARIFYAN Jr

Rostov State Transport University  
2, Rostovskogo Strelkovogo Polka Narodnogo Opolchenia sq.  
Rostov-on-Don, 344038, Russia

\*Corresponding author. E-mail: [kolpahchyan@mail.ru](mailto:kolpahchyan@mail.ru)

## STUDY OF THE ASYNCHRONOUS TRACTION DRIVE'S OPERATING MODES BY COMPUTER SIMULATION. PART 2: SIMULATION RESULTS AND ANALYSIS

**Summary.** The problem arising at the design of electric locomotives with asynchronous traction drive are considered. The electrical scheme provides the possibility of individual (by axle) control of traction motors. This allows realizing the operational disconnection/connection of one or more axles in the automatic mode, with account of actual load.

In Part 1 of this paper, the complex computer model based on the representation of AC traction drive as controlled electromechanical system was developed. The description of methods applied in modeling of traction drive elements (traction motors, power converters, control systems), as well as of mechanical part and of "wheel-rail" contact, was given.

In Part 2, the results of dynamic electromechanical processes modeling in various modes of electric locomotive operation (start and acceleration, traction regime in straight and curve railway sections, wheel-slide protection, etc.) are presented. In perspective, based on the developed model, the evaluation of locomotive's energy efficiency at the realization of various control algorithms must be obtained.

## ИССЛЕДОВАНИЕ РЕЖИМОВ РАБОТЫ АСИНХРОННОГО ТЯГОВОГО ПРИВОДА МЕТОДАМИ КОМПЬЮТЕРНОГО МОДЕЛИРОВАНИЯ. ЧАСТЬ 2: РЕЗУЛЬТАТЫ МОДЕЛИРОВАНИЯ И АНАЛИЗ

**Аннотация.** Рассматриваются проблемы, возникающие при проектировании электровозов с асинхронным тяговым приводом (АТП). В электрической схеме реализована возможность индивидуального (поосного) регулирования тяговых двигателей, что дает возможность оперативного отключения/подключения одной или нескольких осей в автоматическом режиме, с учетом реальной нагрузки.

В части 1 настоящей статьи была представлена разработанная комплексная компьютерная модель, основанная на рассмотрении АТП как управляемой электро-механической системы. Приводится описание методов, использованных при моделировании элементов тягового привода (тяговых двигателей, силовых преобразователей, систем управления), также как механической части и контакта «колесо-рельс».

В части 2, представлены результаты моделирования динамических электро-механических процессов в различных режимах работы электровоза (трогание с места, движение в режиме тяги в прямых и кривых участках пути, подавление боксования и т.д.). В перспективе, основываясь на разработанной модели, должна быть по-

лучена оценка энергетической эффективности электровоза при реализации различных алгоритмов управления.

## 1. INTRODUCTION

A six-axle electric locomotive with individual control of traction motors is considered as a controlled electromechanical system which includes the mechanical part as multibody structure, the electrical part (energy conversion devices and traction motors) and the control block (control algorithms and their realization). The full-size complex computer model, based on the subsystem technique, was presented in Part 1 of this paper.

The energy conversion system provides the operation of the electric locomotive by feeding from catenary network of 3 kV DC and of 25 kV, 50 Hz AC. It is modeled as an electric circuit, which consists of a main transformer, 4q-S input converters, a DC link and self-commutated voltage inverters for feeding the traction motors. The ATM's model is based on the presentation of induction motor as a system of magnet-connected contours.

The two-channel automatic control system with independent control of the rotor flux and electromagnetic torque is developed. The stabilization of rotor flux magnitude in all modes eliminates the excessive saturation of the magnetic system.

The mechanical part of the electric locomotive consists of a car body and three two-axle bogies. The processes during coasting movement was studied, the normal reactions and the forces of interaction in the wheel-rail contact is shown. The frequency response was built for the car body bouncing, pitching and lateral rolling oscillations. Some qualitative features of the dynamic behavior are noted.

In Part 2, the obtained results of dynamic electromechanical processes simulation in various modes of electric locomotive operation are presented.

## 2. SIMULATION RESULTS

With the help of the developed computer model of the electric locomotive, the complex estimation of the control system principles and algorithms, the determination of its influence on the functioning of ATM and power conversion devices and the analysis of electromechanical processes at various operation regimes were executed [3 – 6].

The analysis of the interaction of the ATD with the mechanical part of the locomotive in the traction mode was performed at various operation modes: locomotive's start and acceleration, motion in a straight line and in curves with maintaining speed, appearance and elimination of wheel slide, etc.

### 2.1. Locomotive's start and acceleration

Let us consider the simulation results of electro-mechanical processes in the locomotive during start and acceleration.

The significant magnetic inertia of the ATM and the existing current and voltage constraints from the inverter result in that the simultaneous control of moment and flux linkage with great disagreement is practically not possible. Thereby, the control system sets the preset moment value equal to 0 at the electric locomotive commencing within 0.2 s from the start of operations that is necessary for the termination of the control transience of the rotor flux linkage. Then the preset moment value increases up to the required value at a predetermined rate enabling the avoid once of undesirable phenomena at the locomotive's mechanical part.

Some simulation results are shown in Fig. 1, where:  $U_{AB}$  is the line-to-line voltage of the ATM;  $I_A$  is the phase current;  $M_1^*$ ,  $M_{em1}$  are the preset and realized electromagnetic torques;  $\omega_1$  is the angular

velocity of the first ATM's rotor;  $F_{x1l}$ ,  $F_{x1r}$  are the traction forces for the left and right wheels of the leading wheelset;  $F_{T1}$ ,  $F_{T2}$ ,  $F_{T3}$  are the forces in the traction rods.

Computer animation of the ATM magnetic field is available at [1].

Obtained results show the good dynamical characteristics by take-off. There are no oscillations in the mechanical part of the locomotive. Generally the quality of regulation is quite high within all intervals of loads and velocities, including take-off conditions and high velocity.

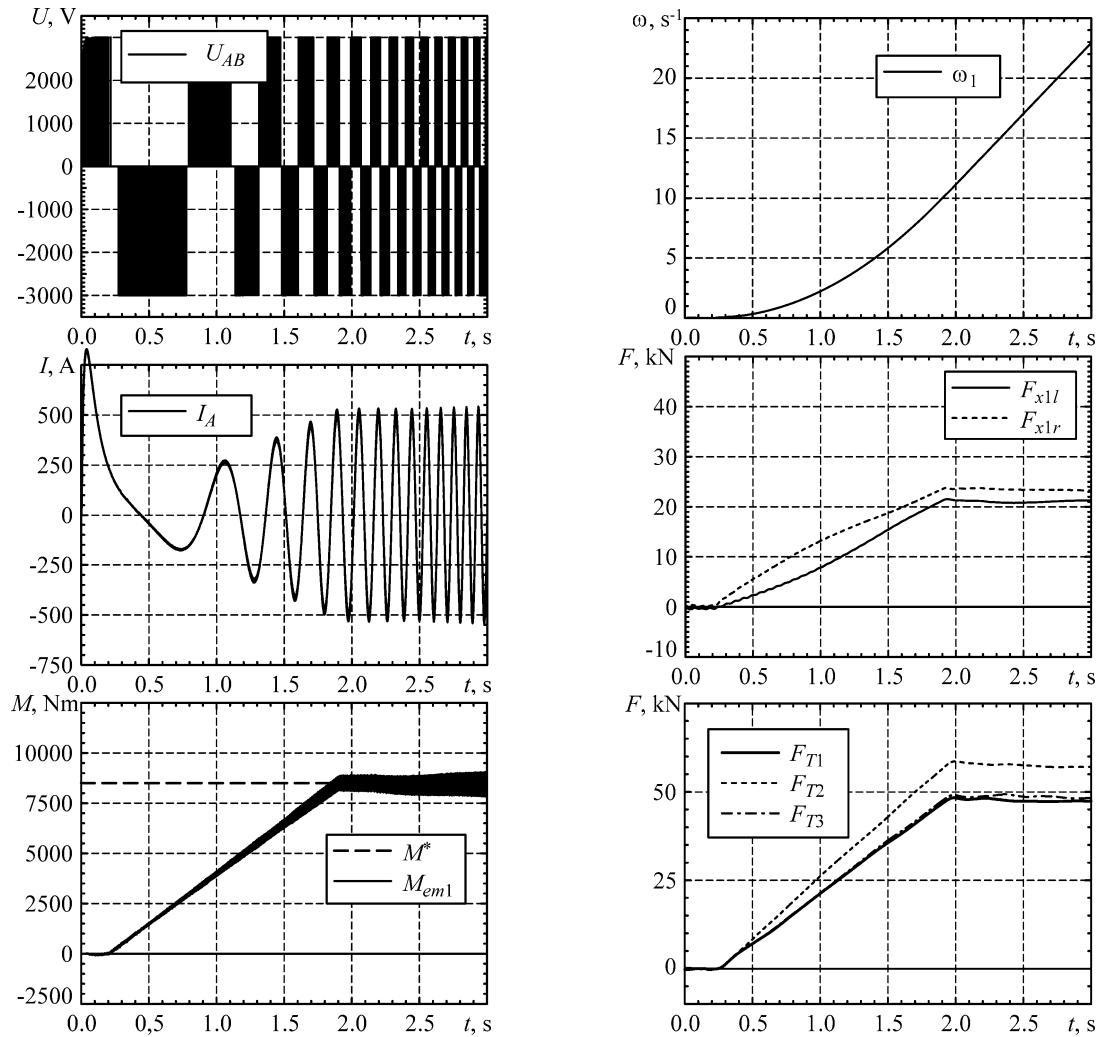


Fig. 1. Electromechanical processes at start and acceleration

Рис. 1. Электромеханические процессы при пуске и разгоне

## 2.2. Movement in traction mode with constant speed on a straight railway section

The calculations were performed for the case when the locomotive is moving at the constant speed of 80 km/h on a straight horizontal railway section. The railway has microirregularities of rails in the vertical and horizontal planes according to the UIC materials. The maximum value of the adhesion coefficient is taken equal to 0.25.

The power is supplied by AC catenary; the electrical part of ATD is modeled in accordance with the Fig. 1 of the Part 1. The obtained graphics of the electromagnetic torques at the ATM shafts of the front bogie ( $M_{em1}$  and  $M_{em2}$ ); of the torques after the rubber-cord coupling ( $M_{rec1}$  and  $M_{rec2}$ ); of rotor angular speeds ( $\omega_{r1}$  and  $\omega_{r2}$ ) and of the angular speeds of wheel sets, reduced to the rotor ( $\omega_{w1}$  and  $\omega_{w2}$ ) are shown on Fig. 2. The corresponding results for the middle and rear bogies were also obtained.

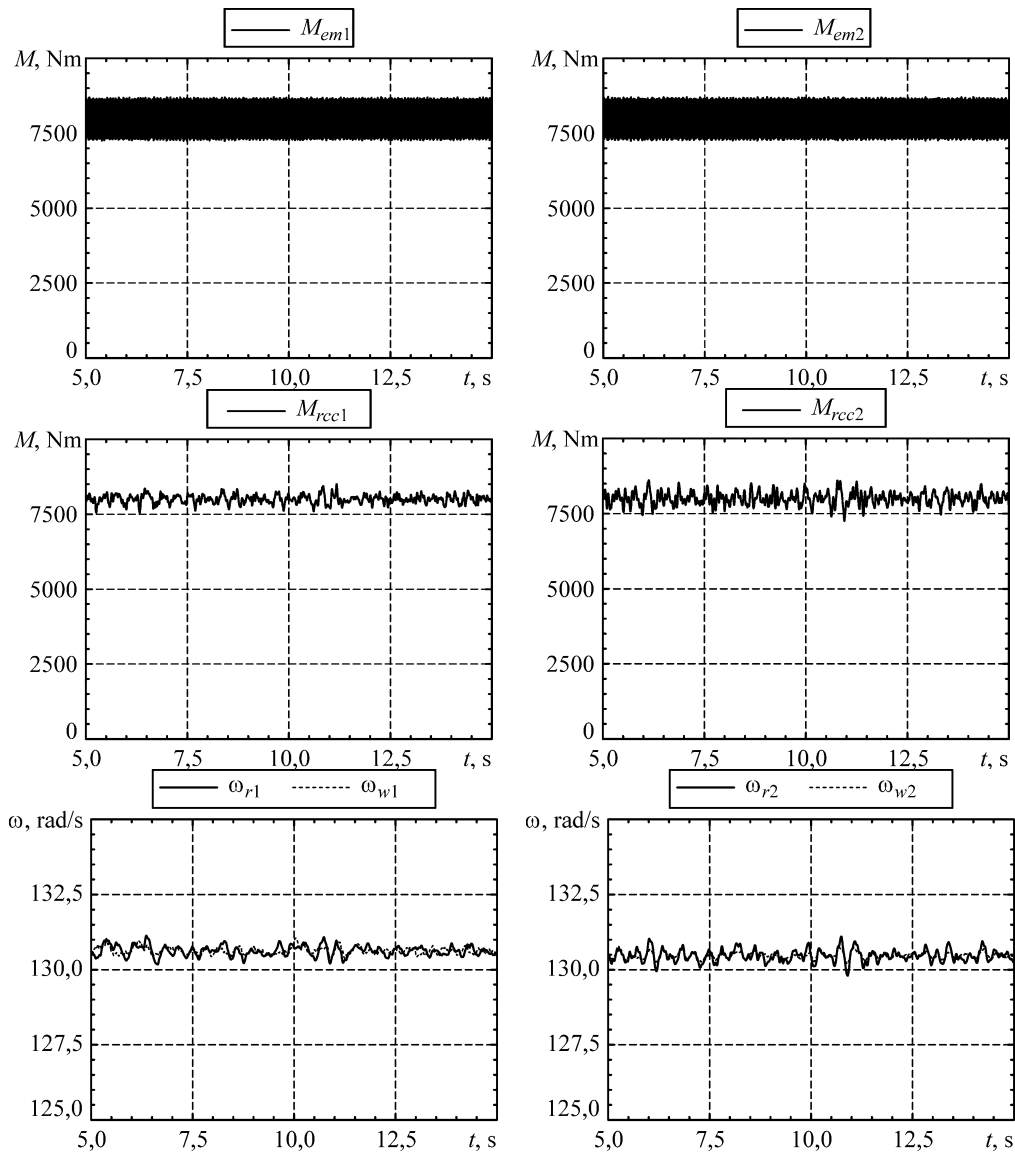


Fig. 2. Dynamic processes at movement in a straight line for the traction mode (top to bottom): torques on the ATM shafts and after rubber-cord couplings, angular speed of ATM rotors and of front bogie's wheel pairs

Рис. 2. Динамические процессы при движении по прямой в режиме тяги (сверху вниз): моменты на валах АД и после резинокордных муфт, частоты вращения роторов АД и колесных пар передней тележки

The formation of inverter output voltage is performed using space-vector PWM (modulation frequency of 1500 Hz). The principle of automatic regulation to maintain the constant rotor flux of ADM is realized. The setting of the flux is taken equal to 3.8 Wb, of the torque – to 8000 Nm, which corresponds to the limit of adhesion.

As can be seen from these results, the high-frequency pulsations of electromagnetic torque on the ATM shaft, arising as consequence of the power feeding from inverter, is almost completely absorbed by the rubber-cord coupling. The low-frequency oscillations of the torque are explained by dynamic processes in the locomotive mechanical part, which are a consequence of the impact of unevenness track structure.

The graphs of vertical forces in wheel-rail contact for the left and right wheels of the first ( $F_{z1l}$ ,  $F_{z1r}$ ) and second ( $F_{z2l}$ ,  $F_{z2r}$ ) wheel sets of the front bogie are shown in Fig. 3.

The traction forces for the left and right wheels of the first ( $F_{x1l}$ ,  $F_{x1r}$ ) and second ( $F_{x2l}$ ,  $F_{x2r}$ ) wheel sets are also shown in this figure.

As a result of dynamic processes occurring when driving on the road with irregularities, the load of the wheelsets on the rails and, consequently, the traction forces, have oscillations, the value of which can reach 20...25% from the mean value of these forces (see also Fig. 5 of the Part 1). The first wheelset is the most unloaded. It is limiting in terms of the use of adhesion conditions.

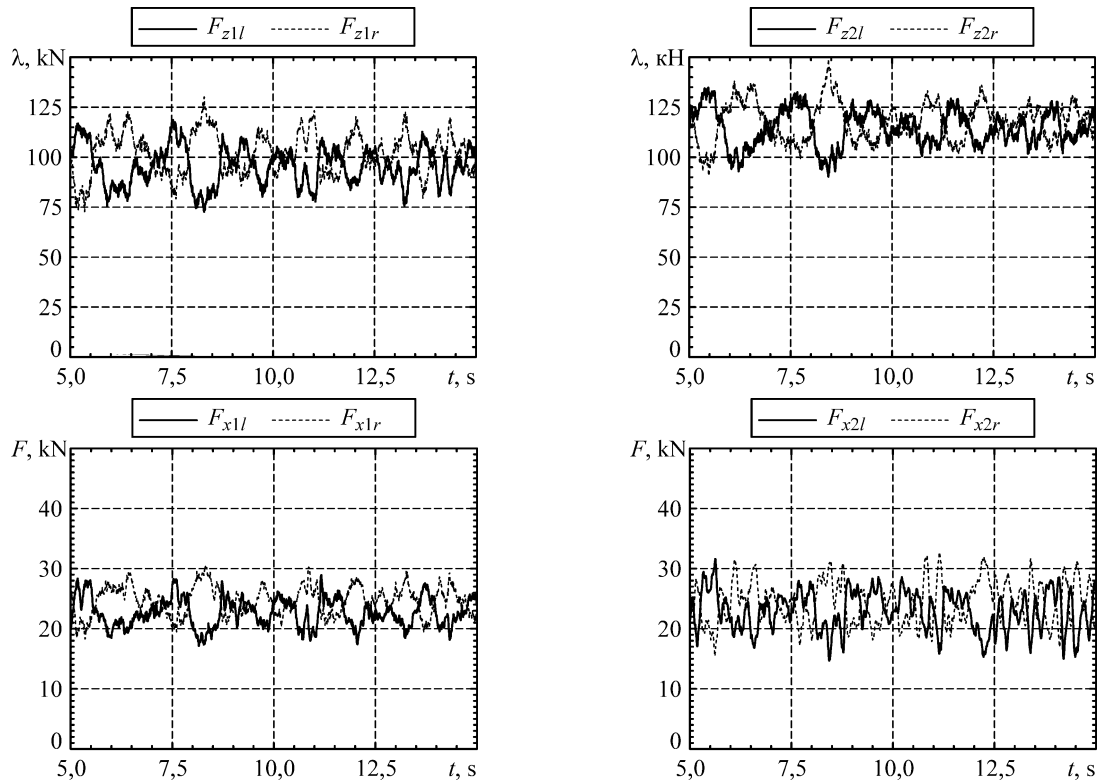


Fig. 3. Dynamic processes at movement in a straight line for the traction mode (top to bottom): vertical forces in wheel-rail contact for the wheel sets of the front bogie; traction forces of the left and right wheels

Рис. 3. Динамические процессы при движении в прямой в режиме тяги (сверху вниз): вертикальные силы в контакте «колесо – рельс» колесных пар первой тележки; силы тяги левых и правых колес

Fig. 4 shows the graphs of the pitching vibrations for car body ( $\varphi_{cb}$ ) and bogies ( $\varphi_{b1}$ ,  $\varphi_{b2}$ ,  $\varphi_{b3}$ ); of the bouncing vibrations for car body and bogies ( $h_{z\ cb}$ ,  $h_{z\ b1}$ ,  $h_{z\ b2}$ ,  $h_{z\ b3}$ ); of the forces in traction rods ( $F_{tr1}$ ,  $F_{tr2}$ ,  $F_{tr3}$ ) and of the total traction force ( $F_{track}$ ).

The efforts in traction rods have the deviation about 20% from the mean value. The reason for this is the pulsations of traction forces at the wheel-rail contacts and the relative movement of the mechanical part's elements. The inertia of the car body and the superposition of these vibrations for three inclined rods smooth the pulsations of total traction force.

In addition to the presented results, the angular and linear displacements of mechanical part's elements, the forces in springs and dampers, the currents and voltages in the electric power conversion system components and in traction motors, the state variables of control system, etc, were calculated.

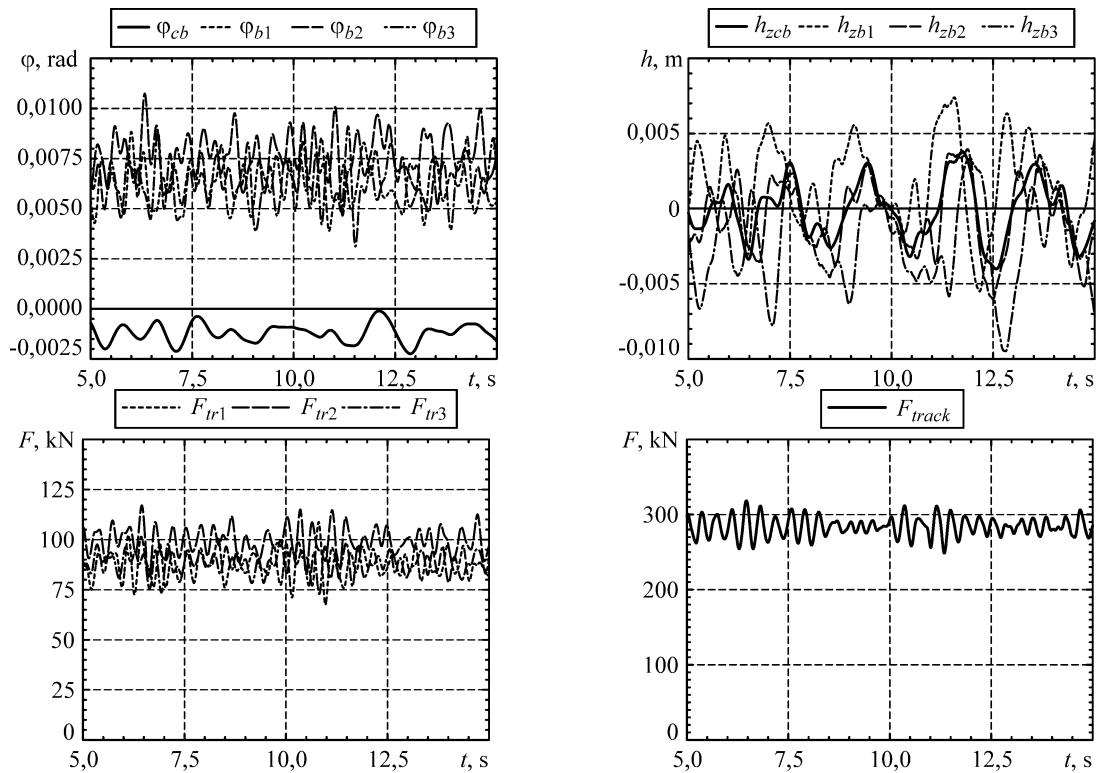


Fig. 4. Dynamic processes at movement in a straight line for the traction mode (top to bottom): pitching and bouncing vibrations for car body and bogies; forces in traction rods; total traction force  
 Рис. 4. Динамические процессы при движении в прямой в режиме тяги (сверху вниз): галопирование и подпрыгивание кузова и тележек, усилия в наклонных тягах, сила тяги

### 2.3. Movement in traction mode with constant speed on a curve railway section

The calculations were performed in the case when the locomotive is moving at the constant speed 80 km/h on a right curve section. The cant (superelevation) of outer rail is  $h = 100$  mm.

The length of the track transition curve is 100 m, the length of the constant radius arc – 300 m. The railway has micro irregularities of rails in the vertical and horizontal planes according to the UIC materials. The maximum value of the adhesion coefficient is taken equal to 0.25.

All parameters of the electrical part and the control system conform to p. 2.2.

The traction torques after the rubber-cord coupling for the first and second axles of the front bogie ( $M_{rcc1}$  and  $M_{rcc2}$ ) are shown in Fig. 5.

The graphs of normal reactions in wheel-rail contact for the first and second axles of the front bogie ( $F_{z1l}$ ,  $F_{z1r}$ ) and ( $F_{z2l}$ ,  $F_{z2r}$ ) are presented in Fig. 6, as shown, for the outer rail the reaction is practically twice greater than for the inner.

The graphs of traction forces for outer and inner wheels of the first ( $F_{x1l}$ ,  $F_{x1r}$ ) and second ( $F_{x2l}$ ,  $F_{x2r}$ ) axles of the front bogie are shown in Fig. 7, the difference is also almost twice. This is explained not only by the fact that the normal reactions of the outer and inner wheels are different, but also by the excess slip for the inner wheel and by the insufficient slip for the outer one.

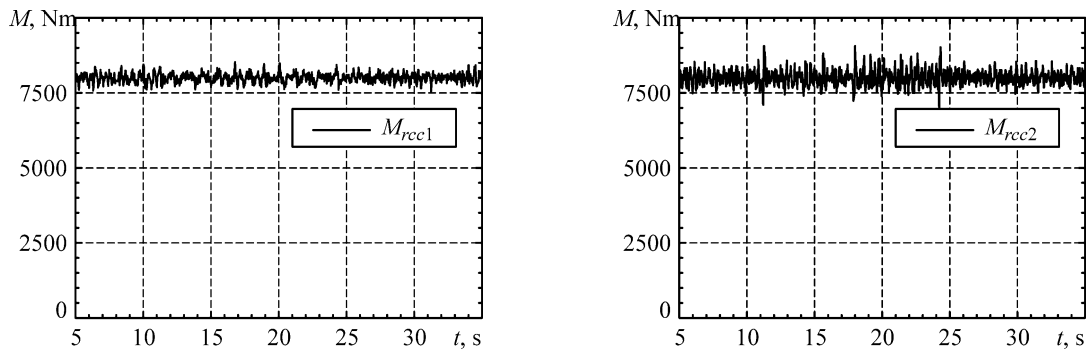


Fig. 5. Dynamic processes at movement in a curve line for the traction mode: torques after the rubber-cord coupling for the first and second axes of the front bogie

Рис. 5. Динамические процессы при движении в кривой в режиме тяги: моменты после резинокордной муфты на первой и второй осях передней тележки

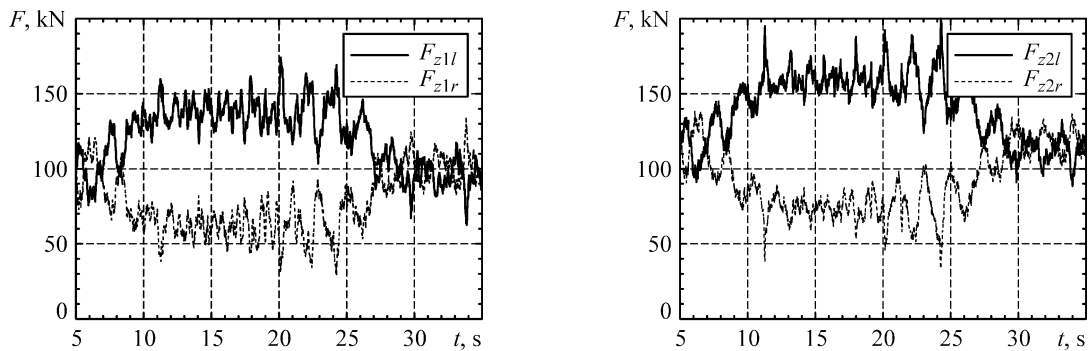


Fig. 6. Dynamic processes at movement in a curve for the traction mode: normal reactions in wheel-rail contact

Рис. 6. Динамические процессы при движении в кривой в режиме тяги: нажатия колес на рельсы

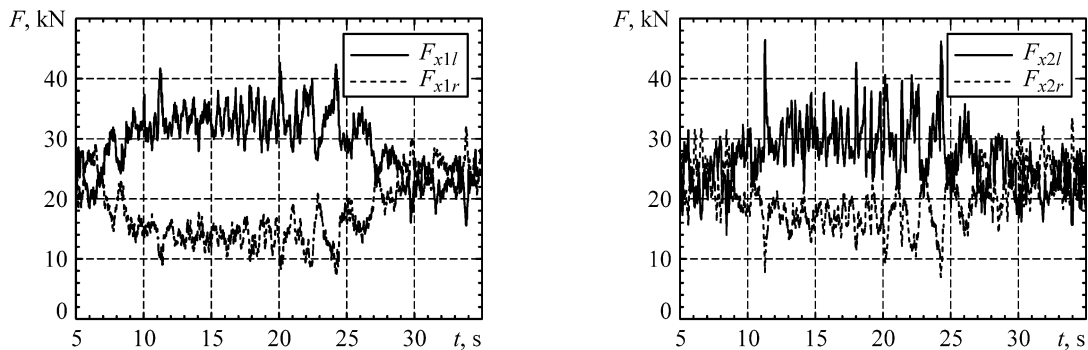


Fig. 7. Dynamic processes at movement in a curve for the traction mode: traction force for outer and inner wheels of the first and second axes of the front bogie

Рис. 7. Динамические процессы при движении в кривой в режиме тяги: силы тяги на колесах первой и второй осей передней тележки

The total lateral efforts for the outer and inner wheels of the first ( $F_{y1l}$ ,  $F_{y1r}$ ) and second ( $F_{y2l}$ ,  $F_{y2r}$ ) axes of the front bogie are shown in Fig. 8. These efforts include both the contact forces in main wheel-rail contact and the strength in the side contact between the flange of the left wheel and the outer rail head's side surface.

As can be seen from the graphs, the bogie moves in the chord position.

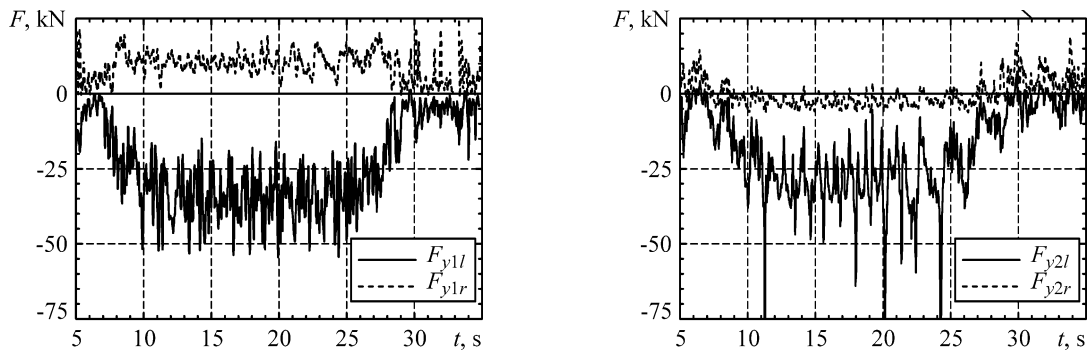


Fig. 8. Dynamic processes at movement in a curve for the traction mode: total lateral efforts for the outer and inner wheels of the first and second axles of the front bogie

Рис. 8. Динамические процессы при движении в кривой в режиме тяги: поперечные усилия на колесах первой и второй осей передней тележки

#### 2.4. The wheel-slide protection system with individual regulation of traction forces

The asynchronous traction drive working at cohesion limit is connected with the high possibility of slippage occurrence. That is why the reliability of the wheel slide protection system mostly determines the efficiency of the ATD control system from the point of view of the most complete utilization of the locomotive coupling weight.

During the investigations, it was found that the wheel-slide protection system should decrease the electromagnetic torque quite smooth preventing impulse loading and oscillations in the mechanical part of the locomotive. Sudden impact of loads arising through unsuccessful control and short-time sliding motion of one or more unloaded wheel sets is possible.

To realize this, the need to implement the individual (by axles) regulation of total traction force.

Let us consider the results of simulation of a wheel-slide protection system by moving the locomotive on a railway section with poor cohesion conditions. The length of the section exceeds the distance between the extreme wheelsets of the locomotive. Vertical and lateral railway track irregularities were taken into account during the simulation.

Simulation results for the first wheel set are shown in Fig. 9. The following designations are used:  $\psi_{ws1}$  is adhesion coefficient in wheel-rail contact of the first wheel set;  $M_{em1}$  is electromagnetic torque;  $\omega_{r1}$ ,  $\omega_{w1}$  are angular velocities of the first ATM rotor and the first wheelset (reduced to the rotor);  $F_{x1l}$ ,  $F_{x1r}$  are traction forces of the left and right wheels;  $F_{tr1}$ ,  $F_{tr2}$ ,  $F_{tr3}$  are forces in the traction rods;  $F_{track}$  is the total traction force.

The obtained results show that decreasing of the adhesion coefficient leads to increasing of angular velocity of the first wheelset. Then the wheel-slide protection system gradually decreases the ATM's torque and the starting slippage is prevented, as is shown in Fig. 9.

When the section with poor adhesion conditions ends, the control system increases the ATM's torque. So, the principles that are implemented in the control system prevent the wheel slipping and provide the good, nearly maximum, value of traction force.

#### 2.5. The control of the voltage inverter at high speed mode

When the locomotive is moving at low or medium speeds, the main harmonic frequency is much greater than the inverter modulation frequency. In these cases, there are no problems with the electromagnetic torque pulsations. The processes occurring at the start of the locomotive are shown in p. 2.1. The medium speed mode was studied in [2].

If the locomotive is moving at high speed, the VI works in one-pulse modulation mode. This can result in high electromagnetic torque pulsation and heat losses. It is very important to reduce the sixth harmonic of the electromagnetic torque pulsations, which is located in the area of the mechanical part Eigen frequencies, which may lead to undesirable resonance phenomena.



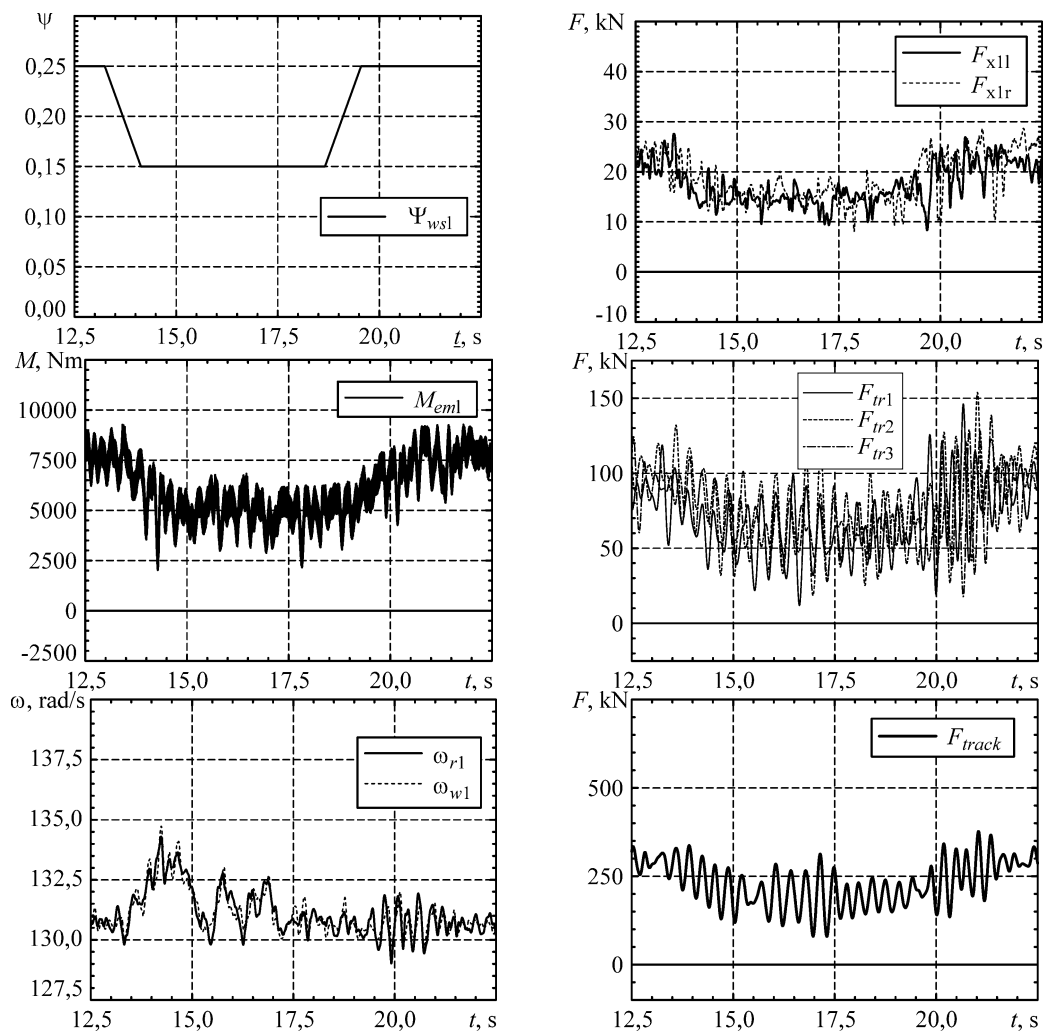


Fig. 9. Passage of railway section with poor adhesion conditions

Рис. 9. Прохождение участка с ухудшенными условиями сцепления

The forming of additional pulses at the beginning and the end of the main pulse reduce the level of these pulsations. The analysis of the electromagnetic torque harmonic composition shown that this solution is effective: the amplitude of the  $6f_1$  harmonic decreases by 40...50%, whereas the amplitude of the fundamental harmonic decreases only of 1...2%.

The simulation results for movement of electric locomotive at 150 km/h are shown in Fig. 10. The power is supplied from the AC catenary. Graphs of voltage and current of the traction transformer winding and voltage of DC-link are shown in Fig. 10, *a*; line-to-line voltage and phase current of ATM – in Fig 10, *b*; the ATM's electromagnetic torque – in Fig. 10, *c*.

The control of energy conversion processes is conducted in such a way that the traction transformer winding current is in phase with the voltage, that the converter consumes the only active power from traction transformer. The voltage in DC-link has a pulsation of significant amplitude with 100 Hz frequency, which is explained by the principle of action of 4q-S converter, which is undesirable due to the influence to the locomotive mechanical part.

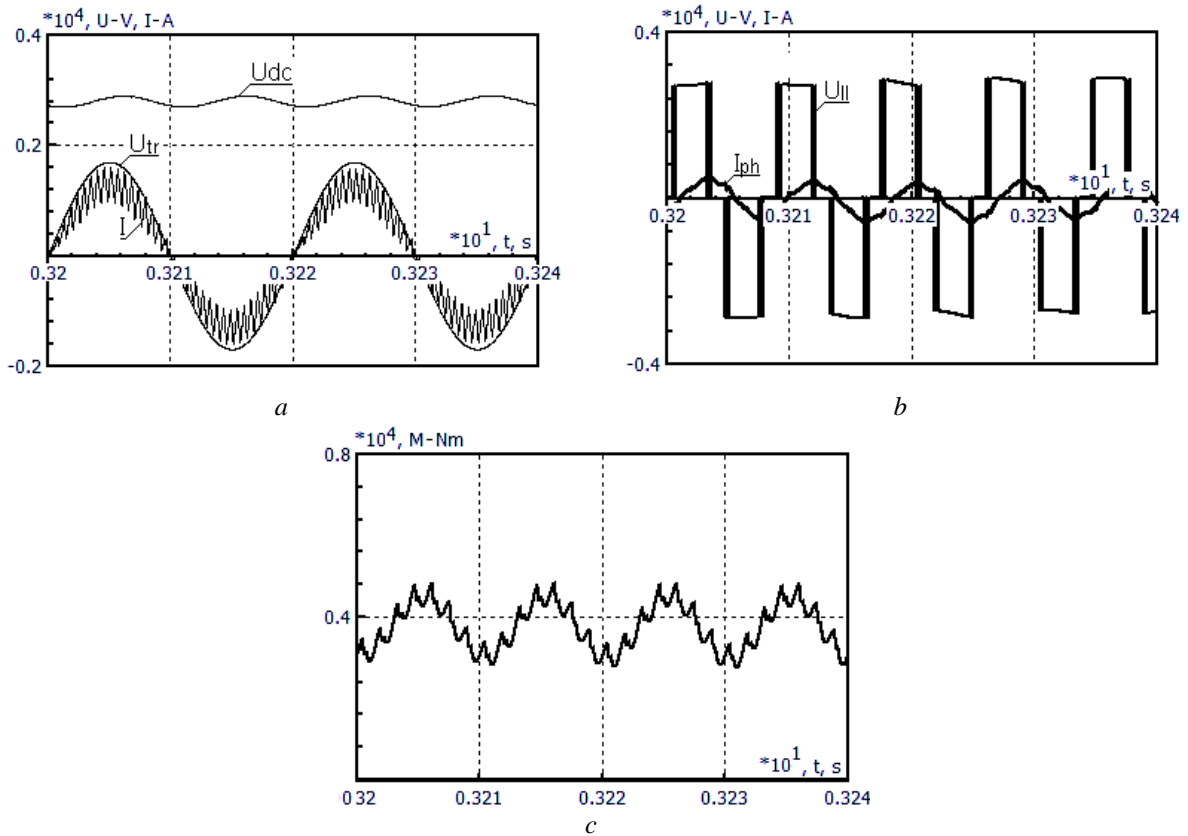


Fig. 10. Voltage and current of main transformer traction wind, DC-link voltage (a); ATM line-to-line voltage and phase current (b); electromagnetic torque (c) at 150 km/h mode

Рис. 10. Напряжение и ток тяговой обмотки трансформатора, напряжение звена постоянного тока (a); линейное напряжение и фазный ток АД (b); электромагнитный момент АД (c) на скорости 150 км/ч

### 3. CONCLUSION AND PERSPECTIVES

The complex controlled electromechanical model of the electric locomotive with ATD was developed in Part 1 of this paper based on the subsystem technique. The model joins the mechanical part, based on a multibody approach, and electric part such as electric circuits.

Complex evaluation of principles and algorithms of the control system of the ATM and analyses of electromechanical processes in the asynchronous traction drive in various working conditions (locomotive's start and acceleration; movement in traction mode with constant speed on a straight and curve railway sections; wheel-slide protection system with individual regulation of traction forces; control of the voltage inverter at high speed mode) were executed in Part 2.

Implemented approaches and software are used for testing automatic control systems and wheel-slide protection systems for newly designed electric locomotives, as well as for the prediction of performances including the transient processes in both mechanical and electric parts.

At present, using the developed mathematical model, are performed the analysis and optimization of the energy conversion system's parameters. Based on the developed model, some variants of the control system are tested and compared.

The electrical scheme allows realizing the operational disconnection/connection of one or more axes in the automatic mode, with account of actual load. In perspective, this approach would lead to improving the locomotive energy efficiency during partial load work.

## References

1. Kolpahchyan, P. *Animation of the asynchronous traction motor magnetic field*. Available at: [https://youtu.be/Fm0\\_an2OPj0](https://youtu.be/Fm0_an2OPj0)
2. Андриященко, А. & Бабков, Ю. & Зарифьян, А. & Кашников, Г. & Колпахчян П. & Перфильев, К. & Петров, П. & Янов, В. *Асинхронный тяговый привод локомотивов*. Москва: УМЦ ЖДТ. 2013. [In Russian: Andrushchenko, A. & et al. *Locomotive's asynchronous traction drive*. Moscow: UMC ZhDT. 2013].
3. Figini, A. & Prone, L. Simulation of the dynamics of railway vehicles: comparison of multibody commercial codes. *Ingegneria Ferroviaria*. 2012. Vol. LXVII. No. 11. P. 897.
4. Diana, G. & Bruni, S. & Corradi, R. & Di Gialleonardo, E. On the derailment of a railway vehicle. Influence of different parameters. *Ingegneria Ferroviaria*. 2012. Vol. LXVII. No. 2. P. 109.
5. Khadri, Y. & Tekili, S. & Daya, E.M. & Daouadji, A. & Merzoug, B. Effects of rail joints and train's critical speed on the dynamic behavior of bridges. *Mechanika*. 2013. Vol. 19. No. 1. P. 46-52.
6. Buksnaitis, J. Analytical determination of mechanical characteristics of asynchronous motors by varying the electric current frequency. *Elektronika ir Elektrotechnika*. 2011. Vol. 17. No. 6. P. 3–6.

Received 21.12.2013; accepted in revised form 02.06.2015